

# The Design and Implementation of a Robot Assisted Crucible Charging System

Vivek A. Sujan and Steven Dubowsky  
Massachusetts Institute of Technology  
Cambridge, MA 02139

Yoshi Ohkami  
Tokyo Institute of Technology  
Tokyo, Japan

## Abstract

A robotic system is developed to automate the packing of polycrystalline silicon nuggets into a fragile fused silica crucible in CZ semiconductor wafer production. The highly irregular shapes of the nuggets make this a difficult and challenging task. In this system, nugget grasping is done with a three-cup suction gripper and nugget manipulation is attained with a 7 DOF SCARA manipulator. An optical 3-D vision system, based on active laser triangulation, measures nugget and crucible profiles. A model-free Virtual Trial and Error packing algorithm determines optimal nugget placement in real time. A hybrid position-force control scheme has been implemented and tested for physical nugget placement. The integrated system achieves high production rates, required precision and cost effectiveness.

## 1. Introduction

The requirements for growing large single device-grade semiconductor crystals are very stringent. Extraordinary low impurity levels, on the order of 1 part in 10 billion, require careful handling and treatment of the material at each step of the manufacturing process. During the CZ semiconductor wafer production process, highly irregular shaped polycrystalline silicon nuggets (Figure 1) are packed into a fused quartz crucibles [5]. The nuggets range in weight from a few grams to about 600 grams. Avoiding contamination, protecting the crucible from damage and following complex packing density rules are key constraints during the process [5]. Currently 18" diameter crucibles, that are packed manually, are being replaced by much larger (more than 36" diameter) crucibles, for use in the upcoming fabrication of a new generation of 300mm diameter wafers. For these crucibles, manual packing is neither ergonomic nor practical. Automation has the potential benefit of reducing cost, achieving greater packing consistency, and reducing packing time. Previous studies have shown that because each nugget has unique size and shape, and strict packing rules, fixed automation was not feasible. The objective of this study was to develop a robotic system to automate this process.

This paper describes the robot assisted crucible charging system developed in this study. There are four key technical challenges for automating the crucible charging process with a robotic system, due to the large variance in size and weight, and the irregular shape of the

nuggets. First, they are difficult to grasp. Second, to pack the crucible, the nugget and crucible surface must be scanned rapidly and accurately to get their profiles. third, the planning system must use this visual information to determine the optimal placement of the nugget in the crucible. Determining the best location to place each nugget is necessary due to the importance of the packing density and complex constraints. Finally, the irregularly shaped and stiff nuggets must be carefully placed against the fragile quartz crucible wall without scratching and contaminating the process. They must also be carefully placed against other nuggets in the process without disturbing the existing structure.

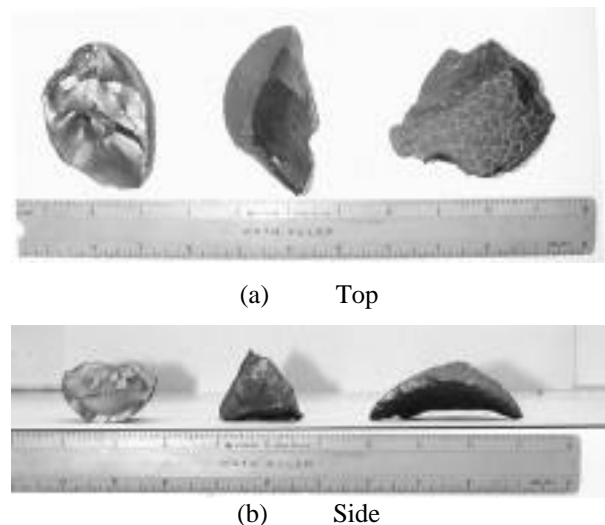
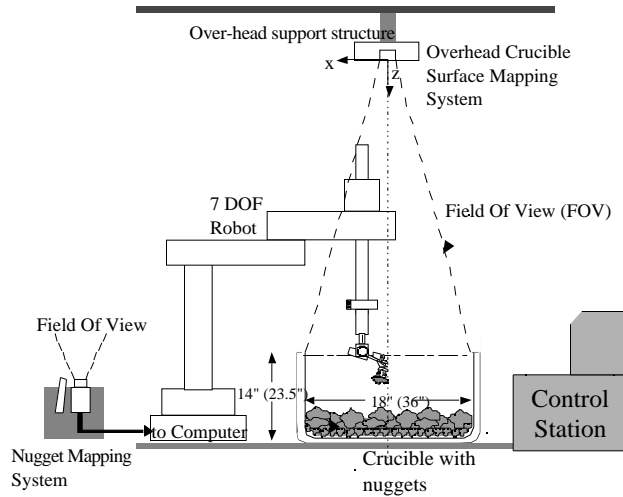


Figure 1 Typical polycrystalline silicon nuggets

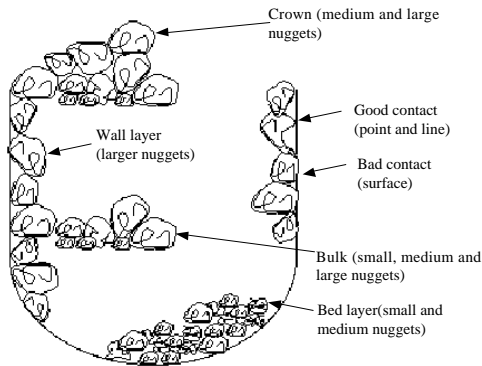
Systems in which robotic manipulators are used to pack objects into a container have been studied previously. Robotic systems have been proposed for the food handling industry and for the bin picking problem using irregular shaped objects [17, 20]. These systems face some of the technical challenges addressed here, however their performance specifications are far less stringent. As these solutions are unable to meet the performance requirements set by the CZ crucible packing task, they are unsuitable for the problem addressed in this paper.

Figure 2 shows the system layout. Packing is initiated with a bed layer formed by "smaller" nuggets, placed using the bulk filler. Packing continues in a stratified manner as larger nuggets are acquired one at a



**Figure 2: Crucible charging system layout**

time and scanned to give a surface profile. Simultaneously, the crucible surface profile is mapped by an overhead vision system. A packing algorithm applies this vision data to compute an ideal position for the nugget. This location is achieved by the 7 DOF manipulator and the nugget is placed. Each nugget layer consists of wall nuggets and internal bulk nuggets (also placed using the bulk filler). Alternate filling of the bulk and wall nuggets eventually provide a full crucible. Finally, packing is completed by a nugget crown (see Figure 3). System timing is extremely important for accurate system coordination. In order to stay competitive with human packing, individual nuggets forming the wall and the crown, need to be placed one every 10 seconds [5]. In such a system, the operator will only be responsible for opening bags and sorting nuggets.



**Figure 3: Typical Crucible with Charging Constraints**

This paper describes the design, integration and calibration of the grasping/manipulation, vision, placement planning and control systems for the robot assisted crucible charging system. A gripper based on vacuum forces for grasping, coupled with a 4 DOF Adept-1 manipulator and 3 DOF wrist, to manipulate the nuggets is described. Two 3-D vision systems using active laser triangulation with CCD cameras, map the crucible and nugget surfaces. An on-line model-free packing algorithm, determines the placement of 3-D irregular nuggets in process constraints and limitations. Using a cost function to determine nugget placement, complex

packing rules and constraints of the CZ process can be readily included in the packing algorithm. Finally, a hybrid position/force control algorithm is developed and implemented on the Adept-1 based laboratory system for regulating the delicate contact forces while in contact with a stiff and fragile environment. Experimental results show the system can meet the requirements for automation of the CZ process.

## 2. Grasping/Manipulation System

### 2.1. System Requirements

The irregular silicon nuggets can be qualitatively divided according to surface shape and quality. Some nuggets have a characteristic mottled surface texture, while others display especially jagged angles. For successful grasping and manipulation, the gripper must be able to grasp at least 85% of the large (80 grams and above) nuggets, grasp the bulk filling bin, and orient nuggets through  $\pm 180$  degrees of yaw and  $\pm 15$  degrees of pitch and roll for arbitrary nugget-wall contact.

### 2.2. End Effector Design

Mechanical gripper designs can be grouped into four classes: clamping grippers, universal grippers, specialty grippers and vacuum/magnetic grippers [6, 22]. Universal grippers are designed to grasp a variety of parts without reconfiguration of the gripper [14, 18]. Both universal and clamping grippers must grasp objects using opposed surfaces. Specialty grippers are often application specific—typically a customized tool. Vacuum and magnetic grippers can pick up parts using one object face. However, magnetic grippers can only lift ferric materials, and vacuum grippers, although promising for their inherent grasping compliance, in only a limited number of cases have been applied toward irregular objects [13]. Due to the highly irregular shaped nuggets, the need for arbitrary nugget to wall contact and other system constraints, vacuum grippers, with inherent grasping compliance, prove to be the most viable solution.

The first step in developing a vacuum gripper is determining the vacuum cup material, size, shape, number, and configuration. Vacuum cup material is selected based on contamination constraints. Vacuum cup size, shape and number determine the maximum lifting force for a given pressure gradient. However, due to the highly irregular shapes of the nuggets, perfect seals are hard to obtain. Hence, vacuum cup geometry must be determined empirically. Vacuum cup geometry can be described using four criteria: the presence of cleats, the shape of the lip, the depth, and the compliance of the vacuum cup. Nugget grasping tests indicate that a bellowed, sharp lipped, non-shallow, smaller vacuum cup is the optimum cup.

The gripper features three closely spaced FDA grade vinyl B3-1 vacuum cups mounted on a manifold plate (Figure 4). This material was found to be least likely to contaminate the packing process. A single vacuum line enters the manifold. Flow to each of the cups is regulated

by three restriction valves in the manifold. Without flow restriction, a single unsealed cup would result in power (pressure) loss to the other cups. A pressure transducer added to the pneumatic lines, measures the vacuum pressure at a point just before the manifold. A successful grasp can then be identified.

The wrist developed for the laboratory houses the gripper and is capable of +30°/-60° of pitch, ±90° of roll, and continuous yaw rotation. Coupled with a 4 DOF Adept 1 manipulator, the 7 DOF system allows for arbitrary nugget placement with respect to the crucible.



Figure 4: Photograph of the End Effector

### 2.3. Experimental Validation

To tune the manifold pressure for a successful grasp with two vacuum seals, a calibration set of 20 nuggets were selected. A maximum downward force of 15 N was used at which point the vacuum cups would bottom out. The flow resistance for a cup was tuned by sealing two cups and adjusting the restriction valve of the open cup until the desired manifold pressure was reached. Figure 5 shows the number of the nuggets successfully grasped as a function of manifold pressure, for both two cup and three cup seal. The greatest number of nuggets was grasped at a vacuum pressure of .76 atmospheres.

This EPS image does not contain a screen preview.  
It will print correctly to a PostScript printer.  
File Name : pressure2.eps  
Title : pressure2.eps  
Creator : MATLAB, The Mathworks, Inc.  
CreationDate : 03/30/98 23:18:50  
Pages : 1

Figure 5: Pressure Test Results

For low manifold pressures (low flow resistance), grasping was unsuccessful in the two cup trials as the unsealed vacuum cup power loss prevented enough pressure from being applied to the nuggets. For the three

cup trials at low pressure, the higher air flow enhanced the ability of three cups to seal onto very rough surfaces of nuggets. At higher manifold pressures, the grasping performance for the three cup gripper fell due to low air flows decreasing sealing ability. Once calibrated for optimum manifold pressure, the gripper grasped 90.9% of all nuggets in one attempt and 98.1% in two grasping attempts.

## 3. 3-D Vision System

### 3.1. System Requirements

The vision system provides the 3-D surface geometry of the individual and the nuggets that have already been packed. The requirements for the prototype crucible surface mapping system design are: X, Y, Z resolution of 1mm, a mapping time of about 4-5s, clearance height greater than the manipulator height and the minimization of blind regions due to obfuscation from crucible walls. In the nugget measurement system, the manipulator carries the nugget over the vision system before it is placed in the crucible. The requirements for the prototype nugget mapping system design are: X, Y, Z resolution of 1mm, and a mapping time of 2-3s.

### 3.2. Vision System Design

To obtain visual 3-D data of an object can be broken down into triangulation, holographic interferometry (phase shift measurement), radar (time of flight), lens focus and Moiré techniques [1, 8, 10]. All these methods suffer some limitations, such as blind regions, computational complexity, limited to highly textured or structured scenes, limited surface orientation, and/or limited spatial resolution [10]. The CZ process contains constraints, such as a complex environment, cost and compactness, which make the practical design of 3-D surface geometry measurement very challenging. To solve this problem laser triangulation was used.

Laser triangulation can be achieved, by a single camera aligned along a Z-axis with the center of the front node of the lens located at (0,0,0) giving the origin of the camera coordinate frame. At a baseline distance b to the left of the camera (along the negative X-axis) a laser projects a plane of light at an angle relative to the X-axis baseline. The point (x, y, z) in the scene is projected onto the digitized image at the pixel (u, v), controlled by the focal length of the lens, f. The measured quantities (u, v) are used to compute the 3-D coordinates (x, y, z) of the illuminated scene point:

$$\begin{bmatrix} x \\ y \\ z \end{bmatrix} = \frac{b}{f \cot(\theta) - u} \begin{bmatrix} u \\ v \\ f \end{bmatrix} \quad (1)$$

The X and Y resolution (X, Y) is given by the width of the projected image onto the detector divided by detector resolution. The depth resolution (Z), given image width W and detector grid size n in pixels, is given by:

$$Z = (W \tan \theta) / n \quad (2)$$

Based on this design and requirements the crucible and the nugget mapping systems outlined in Figure 6 and 7

respectively, were developed. A low resolution global scan of the 18" diameter crucible with XY resolution of 1.5 cm takes one second to process. A high resolution local scan (6" wide band) with XY resolution of 1mm takes 4.5 seconds to process. Laser scanner times are negligible. The nugget mapping system consists of a fixed laser and camera. The manipulator is required to maintain a constant linear velocity of the nugget across the camera FOV of 3 cm/s. Scanning of a nominal nugget (3"x3") takes 2.5s with an XY resolution of 1mm. All times are based on a video frame rate of 30 frames/s. Critical parameters for both systems (such as inter camera-laser distances, camera field of view, incident laser angles etc.) can be determined from a tradeoff study between the system requirements.

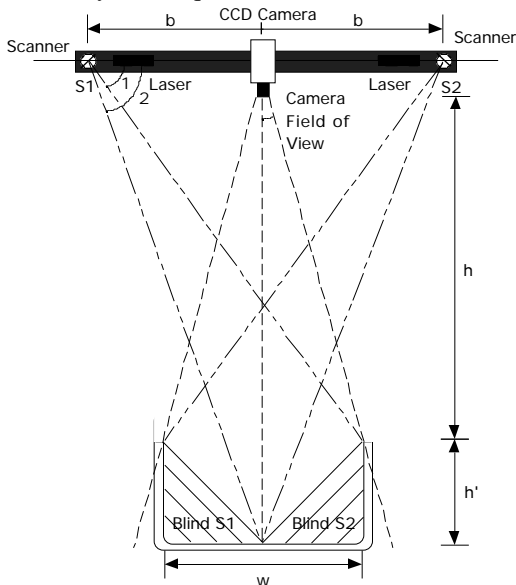


Figure 6: Crucible mapping system design parameters

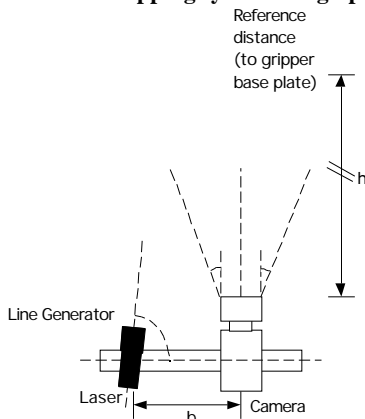


Figure 7: Nugget mapping system design

Finally, the mapping systems must be calibrated to eliminate intrinsic errors (from imperfections in the lens and the detector), extrinsic errors (from uncertainties in inter camera-laser distance and lens focal length) and timing errors (from inaccuracies in frame rates) [5, 8]. Intrinsic errors are eliminated by mapping the errors in image plane coordinates based on known incident light angles. The extrinsic errors are eliminated by scanning a

calibration object at two known angles at the center of the field of view. This yields independent equations in the 2 unknowns that can be solved. Lastly, the timing errors are resolved by online frame rate measurements.

### 3.3. Results

In mapping the nugget field inside the crucible a 15 KHz data acquisition rate is obtained, given a video rate of 30 frames per second and CCD resolution of 500x500 pixels on a Pentium 166 MHz system (see Figure 8 and 9). This yields a mapping time of 4.5 seconds for an 18" diameter crucible with 1mm resolution. Low cost improvements in resolution and computational speeds of the crucible mapping system hardware, can substantially increase this data acquisition rate. The precise measurement of a nugget field to check the crucible mapping system accuracy is difficult. However, estimates of the systems precision indicate that the crucible mapping system meets the required specifications.

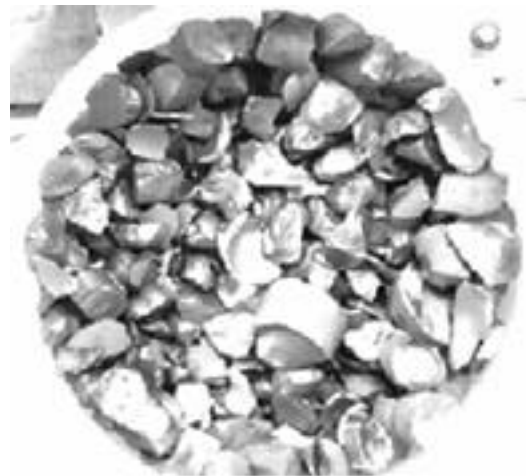


Figure 8: Nugget field image

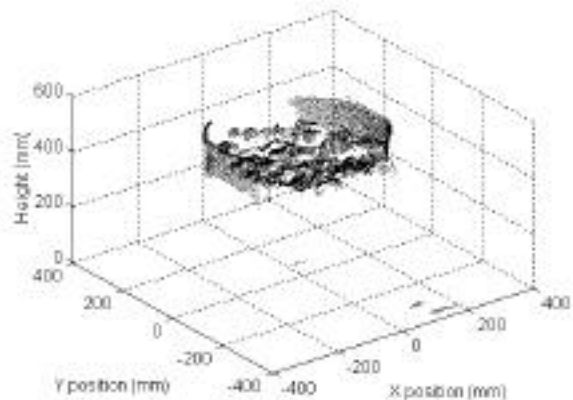


Figure 9: Crucible mapping system nugget field mapped profile

The nugget mapping system was evaluated using representative nuggets. Nugget mapping of a characteristic dimension of 3" and 1mm resolution takes 2.5 seconds based on the 15 KHz data acquisition rate. Nugget maps generated were compared with nugget profiles obtained from Coordinate Measuring Machines. The RMS error between the profiles generated by the two

systems is 0.4mm with of 0.2mm (the accuracy requirement is  $\pm 1.0$  mm).

## 4. Placement Planning

### 4.1. Packing Algorithm Requirements

The crucible is packed in a stratified manner by alternating between placing large nuggets at the wall and center bulk placement. At the crucible rim, nuggets are placed in a conical form to make a crown (see Figure 3). To be economically feasible, the charging system must pack the nuggets at a rate comparable to human operators while following a set of packing rules. The packing algorithm must maximize the packing stability, minimize nugget rejection and optimize the charge density profile. Data provided to the packing algorithm consists of the [x,y,z] maps of the nugget surface and the packed surface. To meet the packing rate, processing time of one second on the control computer is established to determine appropriate nugget placement. The smallest packing search step size is 1mm, defined by the resolution of the vision system

### 4.2. Packing Algorithm

The packing algorithm has an important impact on the charge density, yield and process cycle time. Previous work in 2-D and 3-D packing have been largely focussed on structured objects such as rectangles or rectangular solids respectively [2, 3, 5]. The algorithms developed are largely off-line or on-line processing [3, 5]. To solve the off-line problem, a number of algorithms have been proposed, including dynamic programming, branch and bound, and heuristic search techniques [3, 5, 11]. While they have shown to produce near optimal solutions, they are at best pseudo-exhaustive in nature, computationally intensive and impractical when the number of objects to be packed is large. On-line algorithms, such as genetic algorithms, model-based fitting and simulated annealing, have had some success in packing irregular shaped objects but are computationally intensive [5, 9]. Problem-specific approximation optimization algorithms have also been developed, but are not easily applied to other problems. General methods such as First-Fit decreasing, Harmonic Packing, Level-oriented Packing, with Average-Case and Worst-Case behavior studies, can produce acceptable solutions in reasonable time for a number of applications [11, 21]. However, they typically require object models or complete object geometries. To meet the system requirements in this application, a packing algorithm called “*Virtual Trial and Error*” was developed [5].

The nugget and the internal surface of the crucible are represented by an array of height values in the crucible coordinate frame. Surface voids are identified in the crucible map. The nugget map is transformed to feasible void and the transformation is evaluated by a cost function. Although the exact nugget center of gravity is not known, an estimate for local static stability is performed at the given nugget location (see Figure 10).

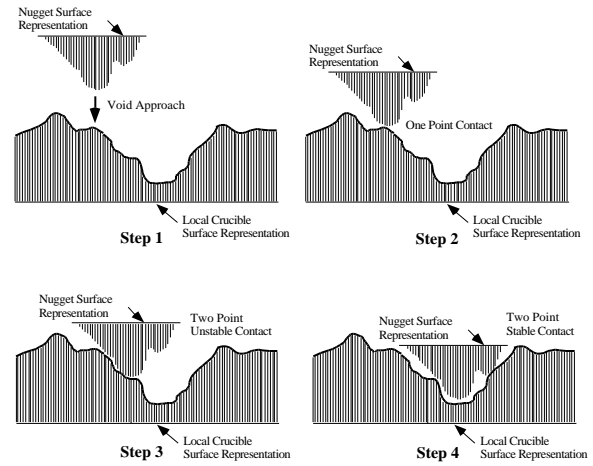


**Figure 10: Finding a locally stable configuration**

Thus the “best” location for the nugget can be identified. This modelless representation leads to a computationally simple algorithm in which changes to the packing rules can be made by simple changes in the cost function. A number of global packing rule primitives have been proposed for packing problems, including [11]:

**Lowest fit** – packing a nugget to lowest position possible.

**Minimum Volume fit** – packing a nugget into a position with least excess volume.

**First fit** – packing a nugget to the first location with excess volume less than some predefined value.

**Contact fit** – packing a nugget into a location with the greatest number of environment to nugget contact points.

A global packing strategy may be one or a combination of several of the above rule primitives. For the CZ packing process, additional packing rules, such as crucible-nugget contact requirements and variable density packing through the charge, can be added directly to the packing strategy. A series of packing strategies were defined and simulations were used to determine the best strategy. Their performance was evaluated based on charge density, the number of nuggets packed successfully out of the number presented and the stability of their placement. The performance index (P.I.) to evaluate the cost function is defined as:

$$P.I. = \frac{d \cdot N_2}{N_1} \quad (3)$$

where  $d$  is the mean charge density,  $N_1$  is the number of nuggets presented and  $N_2$  is the number of nuggets packed and is a measure of stability.

### 4.3. Packing Results

Initial simulations were done for the 2-D version of the problem with six global packing strategies formed from the above packing rule primitives. The nugget shapes are approximated by random non-convex polygons where the size distribution was based on measured nugget data [5]. It was found that the case of lowest fit packing has the

best performance index among the cost functions considered [5]. For the 3-D simulation, the nugget shape is approximated by random polyhedron. Simulation results for packing the walls and crown of the 18" and 36" diameter crucible yielded an average charge density of 48% and 57.5% respectively (with  $\pm 15$  degrees wrist rotations in pitch and roll) using the lowest fit packing rule. With bulk filling, the charge density increases to 50% and 60% respectively. It has been suggested that a controlled variable density through the crucible can improve product quality. The use of this robotic system should provide the consistency to permit this question to be addressed quantitatively. Computational speeds for placement planning are within the 1.0 second per nugget requirement using a PC with Pentium 166 MHz processor. Further, object shape and geometry are not influencing factors in the performance of the algorithm. This compares well with human packing performance.

## 5. Control System

### 5.1. Control System Performance Specifications

Crucible charging involves five distinct subtasks for the control system: nugget acquisition, nugget scanning, slew motion of nugget to crucible, wall and crown building, and bulk filling. The wall and crown building mode is the most challenging of the five control modes. Difficulties arise when the nugget comes into contact with previously placed nuggets. Hence, this section will briefly discuss this aspect of the control. An algorithm must be used which can regulate force and position without *a priori* information of surface orientation. The requirements are as follows:

- Nugget acquisition – vertical motion at 15 cm/s  
Max. vertical force of 15 N
- Nugget scanning – horizontal motion at 3 cm/s  
Max. position error of 0.5 mm
- Slew motion – nugget brought to crucible in 2.5 s
- Wall building – nugget to crucible wall at 10 cm/s  
Max. contact force of 2N
- Bulk filling – bulk filler approaches crucible in 2.5 s  
Filler shaken at 4 Hz with 2° amplitude

### 5.2. Control Algorithms

Two major approaches for both contact force and endpoint position control for manipulators are hybrid position/force control and impedance control [4]. In hybrid position/force control, perfect position tracking can be obtained without the generation of excessive contact forces, making it highly applicable to known stiff environments [19]. However, switching position and force domains during contact can cause instability. Various schemes have been devised which incorporate sensor information to achieve improved endpoint position and force control without introducing the system instabilities [12, 16]. Impedance control employs a dynamic model to create equations of motion of a manipulator [7]. When contact force feedback is incorporated in the model, force control can be achieved.

The advantage of impedance control is its stability and applicability during the entire contact control task. However, this leads to large position errors. In this study hybrid control was developed.

Two hybrid position/force control schemes have been implemented and tested. One performs Jacobian Transpose control in the position domain; the other performs Jacobian Inverse control in the position domain. Both schemes perform Jacobian Transpose control in the force domain.

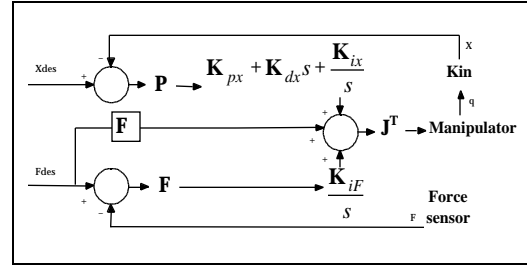


Figure 11: Hybrid P/F Control, J Transpose

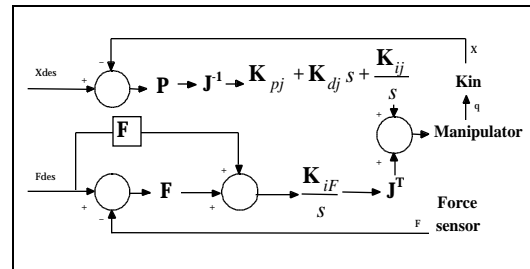


Figure 12: Hybrid P/F Control, J Inverse

Figure 11 shows the implemented Jacobian Transpose hybrid position/force control algorithm. The position domain and force domain are represented by the projection matrix P and the complementary projection matrix F respectively. The joint locations  $q$  are measured and converted via the kinematic equations (Kin) to endpoint position  $x$ . The gains  $K_{px}$ ,  $K_{dx}$  and  $K_{ix}$  represent stiffness, damping, and integration gain in the Cartesian task-space. Figure 12 depicts the control algorithm for Jacobian Inverse position control. This scheme is similar to that shown in Figure 11, but  $K_{pj}$ ,  $K_{ij}$ , and  $K_{dj}$  represent *joint-space* stiffness, integration, and damping gains. It is important to minimize the approach speed so that there is no impact damage to the crucible. It is possible that the manipulator loses contact, and this condition must be handled gracefully by prohibiting the manipulator to achieve high speeds. If the manipulator breaks contact, the integral force controller shown in Figures 11 and 12, is replaced by a velocity damping term and an integral positioning term which brings the manipulator back into contact with the surface slowly.

It is important to note that the P and F selection matrices are likely to change during a contact control task. Before contact, P is the identity matrix (full rank) and F is the zero matrix (no rank). After point contact without friction, the P matrix loses one rank and the F matrix gains one rank. However, due to the integrators locations

as shown, a discontinuous change in P and F does not translate to a large discontinuity in control input.

### 5.3. Results

In order to demonstrate the effectiveness of these algorithms, two-dimensional simulations were performed. The system model consists of a SCARA manipulator arm in contact with a stiff cylindrical crucible. Figure 13 shows the results of an experiment in which the end-effector is commanded to slide along the crucible surface in the  $x$  direction after contact. The desired position is a sinusoid of amplitude 0.02 units and period 6.28 seconds. Note that the amplitude is small enough that the  $y$  position of the trajectory is essentially constant. Contact force is to be regulated at 15N. Contact is detected at 4.5 seconds, and results in a large initial force spike and momentary positioning error. The contact force is then regulated relatively quickly to 15N. There is a lag in the position tracking, which creates a periodic error of about 0.003 units in amplitude.

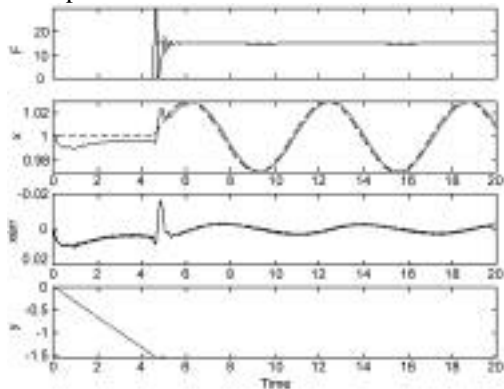


**Figure 13: Simulation Results, Sinusoidal Motion**

Figure 14 shows the results of a trial in which the nugget is commanded to slide in the vertical ( $z$ ) direction while in contact with the wall. The desired contact force is set at 5N to avoid surface scratching. The desired position trajectory is a 0.1 Hz sinusoid of amplitude 1 cm. Contact is detected at approximately one second. The force controller is partly able to maintain the desired force, with deviations ranging from +1N to -2.5N. The position controller maintains the vertical position error to within  $\pm 2$  mm.

The experimental results show that the implemented hybrid position/force control algorithms perform well when the position controller acts as a regulator, and show some success with simultaneous motion and force profiles. In cases where the robot loses contact with the surface, contact is re-established safely. Experimental results suggest that several factors influence the degradation of the controller when generating simultaneous position and force profiles: dynamic coupling in the force/position domains, force sensor cross-talk, joint friction, and over-simplification of the model. To obtain better performance with a hybrid controller, elimination of these disturbances is required.

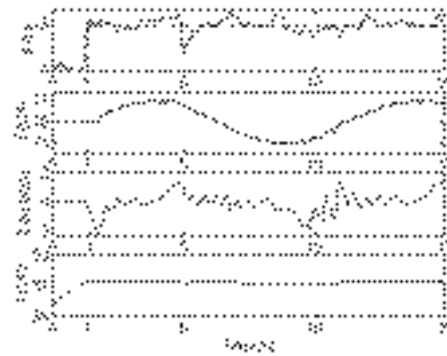


**Figure 14: Adept Nugget Test results, Nugget in Motion**

## 6. Laboratory System Integration

The laboratory system consists of the robot manipulator and control subsystem, vision/packing subsystem, and wrist/gripper subsystem (see Figure 15). The packing procedure plays a supervisory role in planning and assigning control to the major subsystems. This includes nugget acquisition, nugget scanning, crucible surface mapping, placement planning, nugget placement and bulk filling.

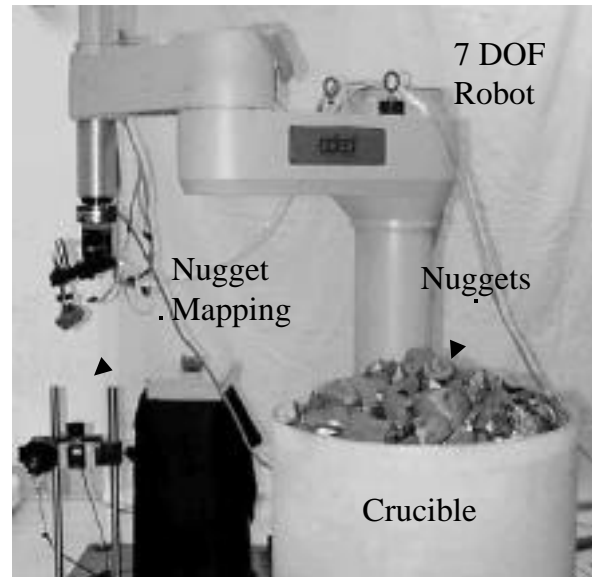


**Figure 15: Experimental system**

In order to provide for accurate scheduling, the governing system communicates with the four major subsystems, either across computers or across programs. It is recommended that the factory level system be operated by a central workstation in order to maintain simplicity. For inter-computer communication, a series of asynchronous handshaking protocols have been developed for communication. The system was implemented and tested on a 166-MHz Pentium computer, using the C++ programming language. The control code is interrupt-driven. The computer system multitasks between two programs: a slow outer loop (which handles subsystem task scheduling and interaction of the system with the user), and a faster time-critical

inner control loop (which processes the encoder information and produces an output control commands for the manipulator/gripper and the vision systems).

Since the crucible charging environment can be damaged rather easily, it is very important to allow user interaction to alter the manipulator's behavior on-line. The system was able to pack nuggets at an average rate of 1 nugget every 10 seconds, reaching a charge density of 50% for the 18" diameter crucibles, allowing the system to stay competitive with human packing.

## 7. Conclusions

A robotic system has been developed to automate the crucible packing process in CZ semiconductor wafer production. The design involves the development of a universal gripper mechanism, non-intrusive nugget and crucible surface mapping modules, a nugget packing algorithm, and control of a manipulator with sufficient compliance and accuracy in the delicate placement of the nugget.

The results of the grasping tests indicate that the designed gripper can perform its required task effectively, with a 98% grasping success at 0.76 atm manifold pressure. Nugget manipulation is attained with a 4 DOF SCARA-type manipulator and a 3 DOF wrist. The non-contact 3-D geometry measuring system based on active triangulation, measures both the nugget geometry profile and the internal crucible geometry profile, with a resolution of 1mm and scanning times of 2.5s and 4.5s respectively. A Virtual Trial and Error packing algorithm is developed and tested in simulation for cost function optimization. The final packing algorithm has been applied in simulation and a charge density of 60% for the 36" diameter crucible is achieved. This compares well with the expected performance of human packing. A hybrid position-force control scheme has been implemented and tested for physical nugget placement. Promising results for simultaneous motion and force profiles have been obtained. The integrated system is seen to achieve charge densities of about 50% for 18" diameter crucibles. Required precision and cost effectiveness has been demonstrated.

## Acknowledgements

The technical and financial support of this work by Shin-Etsu Handotai Co is acknowledged. Also the technical support of Joseph Calzaretta, Anthony Leier, Melissa Tata and Dr. Long-Sheng Yu is appreciated.

## References

[1] Besl, P.J. *Active, Optical Range Imaging Sensors*. Machine Vision and Applications, 1(2):127-152, March 1989.  
[2] Cheng, H.H. and R. Penkar. *Stacking Irregular-Sized Packages by a Robot Manipulator*. IEEE Robotics and Automation Magazine. December 1995. 12-20.  
[3] Coffman, E.G. and P.W. Shor. *Packing in Two Dimensional Asymptotic Average-Case Analysis of Algorithms*. Algorithmica (1993) 9:253-277.

[4] Craig, J., *Introduction to Robotics*, Addison-Wesley, New York, USA 1989  
[5] Dubowsky, S. "Final report on a research program to develop the fundamental technologies for a robot assisted crucible charging system." MIT Internal Report. December 1998.  
[6] Fan Yu, C. "Gripping Mechanisms for Industrial Robots" *Mechanism and Machine Theory*, 17(5), pp: 299-311.  
[7] Hogan, N., "Impedance Control: An Approach to Manipulation," *Proceedings of the American Control Conference*, pp. 304-13, June 1984  
[8] Hsueh, W.J. and E.K. Antonsson. *An optoelectronic and photogrammetric 3-D surface geometry acquisition system*. ASME Winter Annual Meeting on Instrumentation and Components for Mechanical Systems. ASME, November 1992. EDRL-TR 92a.  
[9] Hwang, S-M., C-Y.Kao, J-T.Horng. *On Solving Rectangle Bin Packing Problems Using Genetic Algorithms*. IEEE International Conference on system, Man, and Cybernetics. Humans, Information and Technology. 1994. Vol 2 1583-90.  
[10] Jarvis, R.A. *A perspective on range finding techniques for computer vision*. IEEE Trans. Pattern analysis and Machine Intelligence. PAMI-5(2):122-139, March 1983.  
[11] Li, K. and K.H. Cheng. *Heuristic Algorithms for On-Line Packing in Three Dimensions*. Journal of Algorithms, 13, 589-605 (1992).  
[12] Li, Y.F., "A Sensor-Based Robot Transition Control Strategy," *International Journal of Robotics Research*, Vol. 15, No. 2, pp. 128-136, April 1996  
[13] Mannaa, A.R., Akyurt, M., and El-Kalay, A.K. "Enhanced Gripping Mechanisms for Industrial Robots." *International Journal of Robotics and Automation*, 6(3) pp: 156-160. 1991.  
[14] Mason, M.T. "Manipulator Grasping and Pushing Operations." In *Robot Hands and the Mechanics of Manipulation*. MIT Press, Cambridge, USA. 1985.  
[15] Morel, G. and Dubowsky, S., "The Precise Control of Manipulators with Joint Friction: A Base Force/Torque Sensor Method," *Proceedings of the IEEE International Conference on Robotics and Automation*, Vol.1, pp. 360-365, 1996  
[16] Muto, S. , Shimokura, K., "Accurate Contact Point Detecting Using Force and Velocity Information Complementarily," *Proceedings of the IEEE International Conference on Robotics and Automation*, Vol. 1, pp. 738-744, 1993  
[17] Neal, M.J.; Rowland, J.J. and Lee, M.H. "A Behavior-Based Approach to Robotic Grasp Formulation: Experimental Evaluation in a Food Product Handling Application". *Proceedings of the 1997 IEEE International Conference on Robotics and Automation*. April 1997. pp. 304 – 309.  
[18] Perovskii, A.P. "Universal Grippers for Industrial Robots." In *Robot Grippers* D.T. Pham and W.B. Heginbotham (Eds.) pp: 79-84. Springer-Verlag, NewYork. 1986.  
[19] Raibert, M.H. and Craig, J.J., "Hybrid Position/Force Control of Manipulators," *Transactions of the ASME Journal of Dynamic Systems, Measurement and Control*, Vol. 103, No. 2, pp. 126-133, June 1981  
[20] Trobina, M. and Leonardis, A. "Grasping Arbitrarily Shaped 3-D Objects from a Pile." *Proceedings - IEEE International Conference on Robotics and Automation*, Vol 1 pp: 241-246. May 1995.  
[21] Whelan, P.F. and B.G.Batchelor. Automated packing systems : Review of industrial implementations. SPIE Vol 2064: 358-368.  
[22] Wright, P. and Cutkosky, Mark. "Design of Grippers." In *Handbook of Industrial Robotics*, S. Nof (Ed.), John Wiley and Sons, New York. pp. 96-111. 1985.